



HAL
open science

Modelling tools for ultrasonic inspection of bimetallic welds

Audrey Gardahaut, Karim Jezzine, Didier Cassereau

► **To cite this version:**

Audrey Gardahaut, Karim Jezzine, Didier Cassereau. Modelling tools for ultrasonic inspection of bimetallic welds. Acoustics 2012, Apr 2012, Nantes, France. hal-00811043

HAL Id: hal-00811043

<https://hal.science/hal-00811043>

Submitted on 23 Apr 2012

HAL is a multi-disciplinary open access archive for the deposit and dissemination of scientific research documents, whether they are published or not. The documents may come from teaching and research institutions in France or abroad, or from public or private research centers.

L'archive ouverte pluridisciplinaire **HAL**, est destinée au dépôt et à la diffusion de documents scientifiques de niveau recherche, publiés ou non, émanant des établissements d'enseignement et de recherche français ou étrangers, des laboratoires publics ou privés.



ACOUSTICS 2012

Modelling tools for ultrasonic inspection of bimetallic welds

A. Gardahaut^a, K. Jezzine^a and D. Cassereau^b

^aCEA-LIST, Bâtiment 611 - Point Courrier 120, 91191 Gif-Sur-Yvette Cedex, France

^bEquipe de Statistique Appliquée, 10 rue Vauquelin, 75231 Paris cedex 05
audrey.gardahaut@cea.fr

Modelling tools for the ultrasonic inspection of bimetallic welds, which link ferritic and stainless steel parts, are presented. Those structures are difficult to control as anisotropy, heterogeneity and grain orientation distribution can impede the detection of defects. Dynamic ray tracing is an efficient method to simulate the ultrasonic propagation in welds. The weld can be described as a set of several anisotropic homogeneous domains with a given crystallographic orientation. In this case, the rays travel in straight lines inside each homogeneous domain. Nevertheless, if the domains are small compared to the wavelength and exhibit strong variations in grain orientation, a chaotic behavior of rays may be observed, leading to inaccurate results. To overcome this problem, a smooth description of the grain orientation has to be used. To achieve such a description, the grain orientations are computed on a grid thanks to image processing techniques performed on a macrograph of the weld. In this paper, we first present the state of the art of the welding processes and the weld descriptions. Finally, we describe the image processing techniques that have been implemented.

1 Introduction

Ultrasonic Non Destructive Testing (NDT) is commonly used for the detection, the localization and the sizing of defects located inside or in the vicinity of welds. In particular ultrasonic techniques are used in various industrial sectors (nuclear, petrochemical, etc...) for the inspection of bimetallic welds. Being both anisotropic and heterogeneous, these structures can be difficult to inspect and simulation helpful in order to design inspection, interpret results and demonstrate the performances of the inspection techniques.

The internal organization of grains in the weld depends on the steel shade chosen and also on the parameters of the welding processes like for example the electrode diameter, the welding velocity and the welding technique.

Due to the internal organization of grains in the weld and the characteristics of the media, the detection of defects is complicated as the beam shows disturbances. The effects of splitting or skewing of the beam can be observed on experimental structural echoes [1]. The latter present overloaded intensities along the whole length of the weld and close to the opposite side of the control surface. This is caused by the polycrystalline structure of the weld like anisotropy and heterogeneity.

Various models have been proposed in the literature for the propagation of ultrasonic waves in such anisotropic media. In particular, finite element method has been used by Chassignole and coll. [2, 3] (ATHENA code) to simulate the wave propagation in welds. Alternatively, semi-analytical propagation models based on ray theory have been implemented in the CIVA software [4, 5] and applied to weld inspection. The weld is described as a set of several anisotropic homogeneous domains with a given crystallographic orientation. The rays propagate in straight line within those domains. At each interface, a calculation of the reflected and refracted coefficient is done and the propagation within the next domains is pursued. The results are valid when the domains have dimensions larger than the wavelength and present small variation of impedance between two adjacent areas [6]. If this is not the case, a ray based model on a continuously variable description of the weld has to be used. Such models have been developed in the literature [7]. They are based on the dynamic ray tracing method (DRT) using a smooth description of the grain orientation in the weld. The dynamic ray tracing model for the propagation in anisotropic and inhomogeneous media has been described extensively by Cerveny [8]. Using the transport and Eikonal equations, a differential expression of the ray position and its associated slowness in function of the travel time is obtained. The input data of this model

consists in a description of the material properties of the weld at each node of a mesh.

From the macrograph of the weld, we aim at obtaining by applying image processing two descriptions of the weld; one as a set of several homogeneous domains and another one continuously variable. Those descriptions will be respectively used in the CIVA software as input data of the conventional ray model and of a new dynamic ray tracing model.

In this paper, we first expose the existing methods to get descriptions of welds and their associated models. Then, we present the image processing technique that has been implemented and images obtained on various welds. Finally, we expose the possible improvements of the image processing and the perspectives of this study.

2 Characterization of bimetallic welds

We consider here the inspection of bimetallic welds composed of two shades of steel, a stainless steel and a ferritic steel [9]. During the welding process, a slow cooling leads to the formation of a dendritic structure [10]. At the interface of two beads, the new one remelts the surface of the previous one and the grains borrow the orientation of the existing ones. It is called epitaxial growth. The columnar grains grow along a preferential orientation, the $\langle 100 \rangle$ orientation which is the maximal thermal gradients corresponding to the faster direction of growth. This microstructure is the cause of the anisotropy and inhomogeneity of the weld. Due to the number of parameters in the welding processes, the probability to make two identical welds is really weak. But thanks to macroscopic studies it is possible to better understand the internal organization and to realize a description of a weld [11, 12]. This method is used to obtain a description in several domains considered as homogeneous and orthotropic. The description can be used as input data in the semi-analytical propagation model implemented in CIVA.

A different method allowing to compute the orientation of grains from a visual examination of the metallurgical structure and information from the welding book has been proposed by Moysan and coll. [13]. The orientation of the dendrites in the weld is mapped on a $2 \times 2 \text{ mm}^2$ mesh, chosen as an intermediate scale between the microscopic one (scale of the dendrites) and the macroscopic one (scale of the beads). Alternatively, Ogilvy [14] described the crystalline structure of the dendrites by an analytical law deduced from the observation of macrographs of V-butt weld.

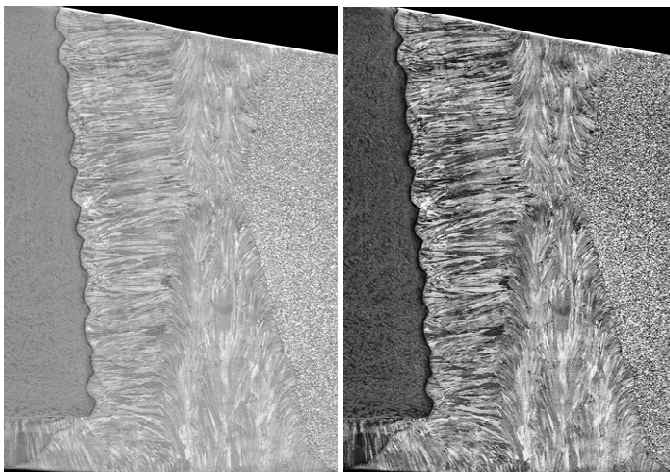
3 Proposed methods for describing welds

We consider simulating the ultrasonic propagation in welds with two different models: the “straight” ray tracing model, compatible with a description as a set of several homogeneous domains, and the dynamic ray tracing model adapted to a continuously variable description of the orientation of the dendrites. The input data of each one of those models is a compatible description of the weld. In this part, we develop the work done in order to obtain two different compatible descriptions of weld from a macrograph with an image processing technique.

From the macrograph, we aim to develop an image processing technique in order to describe the weld as an image of the orientation of the grains. This work was done with the ImageJ [15] software.

3.1 Image processing techniques from the macrograph

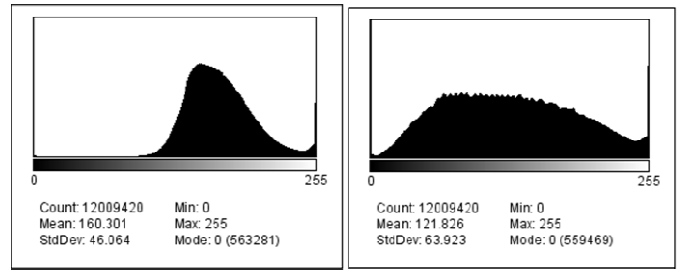
We apply our process on a double-U butt weld with one buttering on the side of the ferritic steel. It is also composed of a cladding as shown in Figure 1(a) in order to protect the ferritic steel from corrosion.



(a) (b)

Figure 1: Images of the studied weld. (a) Original macrograph. (b) Image with equalized histogram.

A macrograph of a bimetallic weld is shown in Figure 1(a). The first operation of the image processing is to enhance its contrast. The image histogram (Figure 2(a)) of the macrograph exposes an irregular tonal distribution. The high intensities are more numerous than the low intensities. In order to increase the contrast of the macrograph, we realize an equalization of the image histogram. The result is shown in Figure 2(b).



(a) (b)

Figure 2: Histograms. (a) Histogram of the macrograph. (b) Equalized histogram

The aim of this process is to spread out the most frequent intensity values on the whole tonal distribution. It consists in an application of a transformation on all the pixels of the image so as to obtain a new one (Figure 1 (b)) with a better redistribution of the intensity values. Comparing the two histograms and the associated images, we notice the enhancement of the contrast.

This “equalized” image enables us to better distinguish the dendrites of the weld but some areas seem to be a little bit blurred especially near the boundary of the weld with the stainless and ferritic steels. Furthermore, the stainless and ferritic steel parts appear to be noisy. With the intention of reinforcing the sharpness of the image, we apply a filter called “unsharp” or “blurred” mask (explanation in Figure 3). It acts on the image at the positions of well-marked edges. It sharpens edges of the image without increasing the noise.

An image considered as the original image (the “equalized” image) is first duplicated. A smoothing is then realized with a Gaussian blur acting as a low pass filter. This second blurred image is subtracted to the first one. The result is the original image with an increase of the sharpness; the edges seem to be more abrupt. This result enhanced high frequencies components of the image. This “unsharp” mask acts like a high-pass filter.

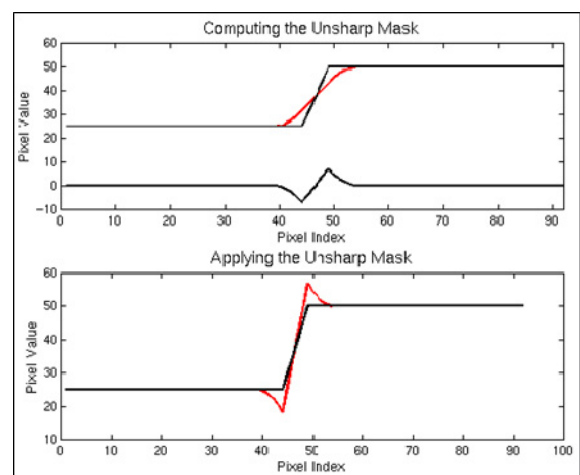


Figure 3: Representation of the “unsharp” mask principle. Top graph: the first black curve represents the intensity value of each pixel on a line of the image. The red curve represents the smoothed duplicated line. The second black curve is the ‘unsharp’ filtered image. Bottom graph: the black curve shows the superposition of the original line and the ‘unsharp’ filtered one.

This filter has two parameters, the radius and the mask weight. The radius corresponds to the standard deviation of the Gaussian blur; it represents the number of pixels affected by sharpening on either side of an edge. The larger the radius is, the more the contrast is increased. The mask weight (0.1-0.9) is the strength of filtering. The edge enhancement is more important for a large strength.

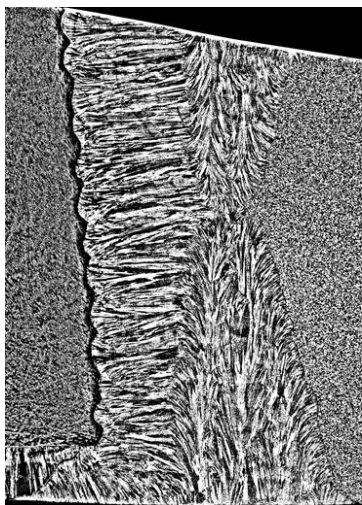


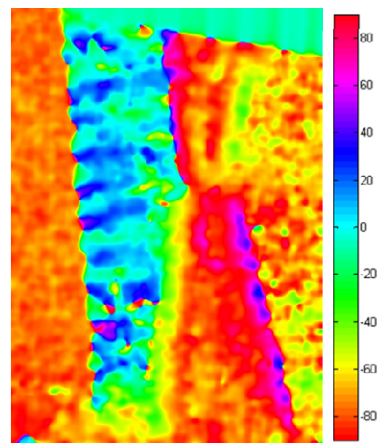
Figure 4: Image with the filter “unsharp” mask.

We choose to apply this mask with the higher possible weight, as to get the better enhanced image, and a length of a quarter of the wavelength. The size of the filter must not be too large in order to enhance small-scale details and avoid the apparition of halos at edges. The final image represented in Figure 4 shows dendrites more enhanced than before and the boundaries of the weld are sharper.

3.2 Computation of the local orientation

The last step of the process is the calculation of the orientation of the dendrites. We use one of the functionalities of an ImageJ plugin called OrientationJ [16]. Based on the evaluation of the structure tensor in a local neighbourhood, the plugin helps us to determine the orientation of every pixel of an image. The algorithm consists in applying a Gaussian-shaped window on the image. As for the “unsharp” mask, we define the size of the window in function of the wavelength. Then, the structure tensor is evaluated for each pixel of the entire image by sliding the Gaussian window. Finally, the program computes a colour image of the local orientation properties. The size of the window of a filter depends on the wavelength. For the “straight” ray tracing model, we want to be able to describe the weld as a set of several homogeneous domains.

The size of the Gaussian window has to be chosen carefully. Thus, we choose a Gaussian-shaped window with a length of a quarter wavelength for the description in domains as it is shown in Figure 5. From this result, we can describe the weld as a set of homogeneous domains (Figure 6).



(a) (b)

Figure 5: Image of the local orientation of the dendrites.

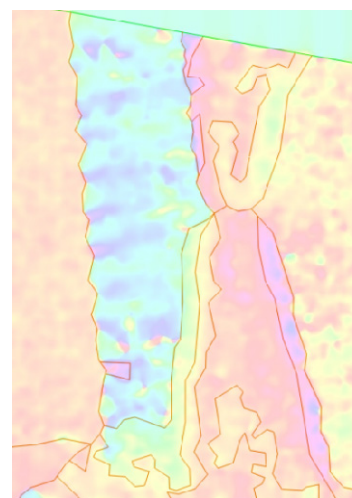


Figure 6: Superimposition of the image of the local orientation and the description in domains.

For the dynamic ray tracing model, we aim to obtain a continuous description of the orientation of the dendrites; so the window has to be chosen so as to ensure a slowly varying orientation with respect to the wavelength. So we choose a Gaussian-shaped window with a length of a half wavelength. The result is shown in Figure 7.

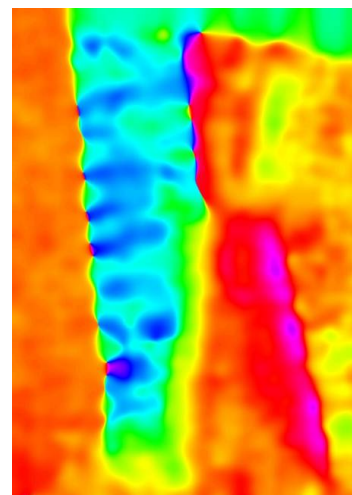


Figure 7: Image of the local orientation for the continuously variable description of a V-butt weld.

The aim of the process is to describe the orientation of the grains in the entire image for every type of welds. For example, we applied it on a V-shaped butt weld composed of a buttering and a cladding area in the side of the ferritic steel. The result of the process is shown in Figure 8.

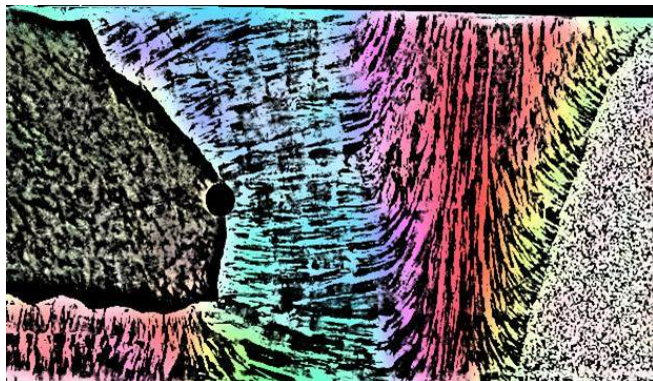


Figure 8: Representation of the superimposition of the image after applying the “unsharp” mask and the calculation of the local orientation of the dendrites.

3.3 Automation of the process

We have exposed an image processing technique for describing the orientation of the dendrites of a weld from its own macrograph. The description for a continuously variable orientation is automatic and the result can be used as an input data for a dynamic ray tracing model. However, the description as a set of several homogeneous domains is not totally automated. The process technique depends on the operator. Thus, this work has to be pursued with the intention of separating automatically the weld in several homogeneous domains.

4 Simulation of weld inspection in CIVA

The ray-based model (pencil model [5]) implemented in CIVA deals with heterogeneous and anisotropic material. In this case, ray paths are straight lines. The results are valid for domains with dimensions larger than the wavelength presenting a weak acoustic impedance contrast. Figure 9 represents the beam in a V-butt weld with a description as a set of several homogeneous domains observed in 3.2.

The extension to smoothly inhomogeneous anisotropic media has been proposed in [17] for simulating the propagation of ultrasonic waves in curved composite components. To achieve this, the model has to deal with a continuously variable anisotropy. It is based on a ray calculation for an inhomogeneous medium using an iterative time-step method. This method consists in solving for each time step a system of differential equations taking into account the continuous anisotropic orientation variation along the trajectory.

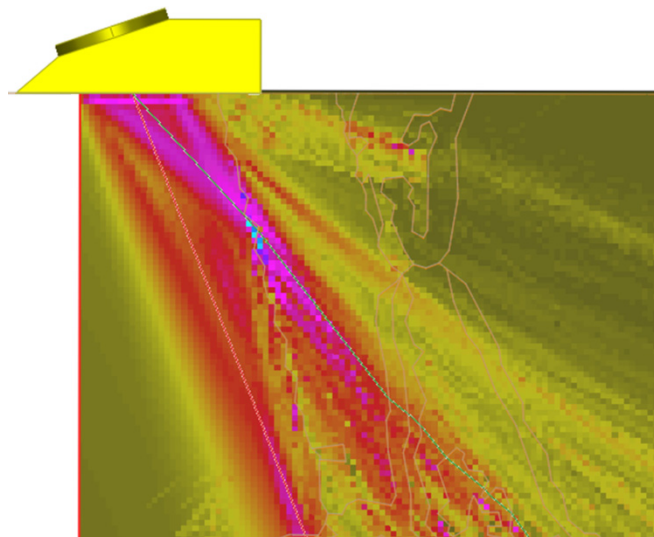


Figure 9: 2D beam visualization in a V-butt weld with CIVA

This dynamic ray tracing model has been described by Cerveny [8]. Using the Eikonal equation and the Christoffel equation, a differential expression (Eq. 4) of the ray position \vec{x} and its associated wave slowness \vec{S} with the travel time of the ray T is obtained:

$$\begin{cases} \frac{dx_i}{dT} = c_{ijkl} S_l P_j P_k = V_e \\ \frac{dS_i}{dT} = -\frac{1}{2} \frac{\partial(\rho^{-1} c_{jklm})}{\partial x_i} S_k S_n P_j P_l \end{cases}, \quad (1)$$

where c_{ijkl} is the elastic stiffness tensor, P_i are the components of the normalized polarization associated to the ray mode, ρ is the density and \vec{V}_e is the energy velocity. This model will be applied on the continuously variable descriptions of bimetallic welds previously obtained.

5 Conclusion

In this communication we have presented image processing technique developed for describing bimetallic welds. The motivation of this work is to obtain a description of the orientation of the dendrites of bimetallic welds from a macrograph. The image processing can be adapted with the intention of getting two different descriptions of the weld (a set of several inhomogeneous domains with privileged orientation and a continuously variable description of the orientation). Results for two types of bimetallic welds have also been shown. The descriptions will be used as input data for two different models of propagation: a conventional ray tracing model and a dynamic ray tracing model.

References

- [1] F. Ahmed, "Etude de la diffusion des ondes ultrasonores dans les soudures auténo-ferritiques: Application à la caractérisation des échos de lignes observés lors du contrôle des soudures bimétalliques", Thèse de Doctorat, 177p, CEA Saclay (1999)
- [2] B. Chassignole, V. Duwig, M.-A. Ploix, P. Guy, R. El Guerjouma, "Modelling the attenuation in the ATHENA finite element code for the ultrasonic testing of austenitic stainless steel welds", *Ultrasonics* 49, 653-658 (2000)
- [3] A. Apfel, J. Moysan, G. Corneloup, T. Fouquet, B. Chassignole, "Coupling an ultrasonic propagation code with a model of the heterogeneity of multipass welds to simulate ultrasonic testing", *Ultrasonics* 43, 447-456 (2005)
- [4] CIVA software platform for simulating NDT techniques (UT, EC, RT) <http://www-civa.cea.fr>
- [5] A. Lhémy, P. Calmon, I. Lecœur-Taïbi, R. Raillon, L. Paradis, "Modeling tools for ultrasonic inspection of welds", *NDT&E Int.* 37, 499-513, (2000)
- [6] J. Brokesova, *Asymptotic ray method in seismology: a tutorial*, Matfyzpress (2006)
- [7] Q. Liu, H. Wirdelius, "A 2D model of ultrasonic wave propagation in an anisotropic weld", *NDT&E International* (40), 229-238 (2007) J.R. Tomlinson, A.R. Wagg, M.J. White, "Ultrasonic inspection of austenitic welds", *British Journal of NDT* 22(3), 119-27 (1980)
- [8] V. Cerveny, *Seismic Ray Theory*, 1st Ed. Cambridge: Cambridge University Press (2001)
- [9] D.S. Kupperman, K.J. Reimann, "Ultrasonic wave propagation and anisotropy in austenitic steel weld metal", *IEEE Trans. Sonics Ultrason.* SU-27(1), 7-15 (1980)
- [10] J.R. Tomlinson, A.R. Wagg, M.J. White, "Ultrasonic inspection of austenitic welds", *British Journal of NDT* 22(3), 119-27 (1980)
- [11] B. Chassignole, D. Villard, M. Dubuget, J.-C. Baboux, R. El Guerjouma, "Characterization of austenitic stainless steel welds for ultrasonic NDT", *Rev. of Prog. in QNDE* 19, 1325-1332, Montréal (2000)
- [12] B. Chassignole, "Influence de la structure métallurgique des soudures en acier inoxydable austénitique sur le contrôle non destructif par ultrasons", Thèse de Doctorat, 217p, INSA Lyon (2000)
- [13] J. Moysan, A. Apfel, G. Corneloup, B. Chassignole, "Modelling the grain orientation of austenitic stainless steel multipass welds to improve ultrasonic assessment of structural integrity", *Int. J. Pressure Ves. Piping* 80(2), 77-85(2003)
- [14] J.A. Ogilvy, "Computerized ultrasonic ray tracing in austenitic steel", *NDT International* 18(2), 67-77 (1985)
- [15] ImageJ : Image Processing and Analysis in Java, <http://rsbweb.nih.gov/ij/>
- [16] OrientationJ : ImageJ's plugin for directional analysis in images, Biomedical Imaging Group, Ecole Polytechnique Fédérale de Lausanne (EPFL), <http://bigwww.epfl.ch/demo/orientation/>
- [17] S. Journiac, N. Leymarie, N. Dominguez and C. Potel, "Simulation of ultrasonic inspection of composite using bulk waves: application to curved components", *Journal of Physics: Conference Series* (2011)